Journal of Applied Fluid Mechanics, Vol. 10, No. 3, pp. 947-955, 2017.
Available online at www.jafmonline.net, ISSN 1735-3572, EISSN 1735-3645.
DOI: 10.18869/acadpub.jafm.73.240.26446

Numerical Studies to Predict the Impact of Air Nozzle Position and Inclination on the Performance of Downdraft Gratifier

P. C. Murugan and S. Joseph Sekhar†

Department of Mechanical Engineering, St. Xavier's Catholic College of Engineering, Kanyakumari District, Tamil Nadu, 629003, India

†*Corresponding Author Email: josephsekhar@hotmail.com*

(Received April 22, 2016; accepted January 8, 2016)

ABSTRACT

Biomass gasification is one of the promising technologies to produce energy from the renewable energy sources, and the downdraft biomass gasifier is a widely used biomass energy conversion device. Among the various components of a gasifier, the position and the inclination of air nozzle have a vital role in the generation of producer gas. Therefore, a proper design is needed to fix the position and angle of the air nozzle. Keeping the above aspects, the present work focuses on the numerical simulation to predict the appropriate position and inclination of the air nozzle in a 50kWth imbert type downdraft gasifier by the species transport approach. The nozzle inclination varies from 0°, 20°, 30°, 45° and 60°, and the nozzle position is considered from 50mm, 100mm, 150mm and 200mm respectively. Experiments were also conducted to validate the numerical study. Both the studies show that the nozzle inclination at 45° and its position at 100mm above the reduction zone gives a reasonable composition of producer gas.

Keywords: simulation; air nozzle; gasifier; rubber seed kernel shell; higher heating value; CFD.

NOMENCLATURE

CFD	computational fluid dynamics	RNG	renormalize group
E	activation energy	Sm	mass added to the phase
h_j	enthalpy of species j	X	species of the reaction
HHV	Higher Heating Value		
I	species i	ρ	density
Nm^3	normal cubic metre	$\tau^{=}$	stress tensor
p	partial pressure of gas species	λeff	effective conductivity
P	product of the reaction	ε	turbulent dissipation rate
R	reactant of the reaction	μ	dynamic viscosity
R	ideal gas constant	Φ	equivalence ratio
R(i,r)	homogeneous reaction rate		

1. INTRODUCTION

As we move towards finding an alternative solution for global warming, climate change and depletion of fossil fuels, biomass is the most promising renewable energy source to tackle the challenges. Also, the intensifying energy cost and environmental impacts of various energy conversion technologies lead to biomass gasification as an important area of research. Many mathematical and experimental studies were already conducted on the biomass gasification technology. Avdhseh Kr. Sharma (2011a) proposed a mathematical model for downdraft gasifier using EQB model and predicted that the reaction temperature in the reaction zone influences the quality of combustible gases. High temperature and pressure are the important factors that cause the pressure drop inside the gasifier. Babu and Pratik (2006) studied that the reduction zone of downdraft gasifier is simulated by incorporating the char reactivity factor and noted that the rate of reaction becomes negative when the temperature falls below 933K. A dynamic response simulation is modelled by Zhiwei *et al.* (2011) for a slagging entrained flow gasifier and they predicted that the temperature distribution is well suited for membrane wall gasifier.

Zainal *et al.* (2001) developed an equilibrium model to predict the performance of downdraft gasifier and calculated the calorific value against the moisture content from the ultimate analysis of the feedstock. Avdhesh Kr Sharma (2008b) developed an equilibrium model for the reduction zone and discussed the operating parameters of the gasifier such as moisture content, pressure, equivalence ratio and producer gas composition. The temperature distribution of the updraft gasifier with babul wood as feedstock has been simulated by Bin Li *et al*. (2013), and the height of gasification zones was calculated. Laurence *et al*. (2012) used gas treatment unit to filter the unwanted impurities (particulate matter, tar and some other impurities) present in the syngas gas generated by the gasification process, which is further used in IC engines.

Luc *et al*. (2008) investigated the oxidation zone of the gasifier and showed that the air injector design and air velocity are the fundamental parameters to control the gasification. A one-dimensional steady state model proposed by Chih *et al*. (2008) predicts the conversion rate from the fuel moisture content and air/fuel ratio. It is also observed that the fuel moisture content will decrease the fuel conversion rate. The model proposed by Yang *et al*. (2005) shows that the stoichiometric air ratio increases with the particle size of the biomass. The updraft gasifier using high-temperature agent gasification with preheated air at 900°C was investigated by Duleeka *et al*. (2014), and showed that the cold gas efficiency and quality of producer gas are influenced by the equivalence ratio. The pyrolysis zone of a gasifier was modelled by Jaojaruek and Kumar (2009) using the lumped heat analysis method, and the model used chemical kinetics to predict the gas composition when the combustion attains pyrolysis temperature.

The co-gasification process was modelled by Zhao *et al*. (2006) using ASPEN plus with a sensitivity analysis approach. The results show that the oxygen has a vital role on the syngas composition. By maintaining the appropriate O_2/fuel ratio, maximum values of the producer gas could be obtained. Carlos *et al*. (2003) developed an equilibrium model to investigate the gasification of saw dust and found that the model is more suitable for the temperature above 1500K. Maria *et al*. (2010) reviewed the various gasification models and reported that the composition of producer gas depends on the fuel composition, operating pressure, temperature, moisture content and the gasifier design. The study also shows that the equilibrium models are less intensive than kinetic models in terms of accuracy in the results. Christus *et al*. (2014a) developed a two-zone kinetic equilibrium for the feedstock such as coir pith, rubber seed kernel shell, wood and coconut shell. It is found out that the rubber seed kernel shell can be used a fuel when other feedstock are in scarcity. Christus *et al*. (2016) studied the performance of the downdraft gasifier with blends of coconut shell and rubber seed kernel shell and predicted that the equivalence ratio should be maintained between 0.2-0.3 for obtaining maximum conversion efficiency.

The numerical studies of Fletcher *et al*. (1997), using Reynolds stress and k- ε models in CFX 4.0, for studying the coal particle behaviour in an entrained flow gasifier suggests that the effect of gasifier height could be optimized. The mixture fraction model has been effectively used to study the gasification of lignite for three nozzle positions (Keran *et al*. 2013). A CFD model (Fletcher *et al*. 2000) in CFX 4.0 package used to predict the performance of entrained flow gasifier shows that the gasification reactions are not sensitive to the velocity field around the particles. The two-stage up-flow and single stage down flow gasifiers were modelled using DPM (Andrew *et al*. (2010)) to predict the temperature, species concentration and the particle trajectories of the entrained flow gasifier.

The design of biomass thermochemical conversion systems are reviewed by Yiqun and Lifeng (2008), and they illustrate that CFD is a very powerful tool for analysing the gasifier and predicting the temperature and flow distribution of gasification products. A CFD model is developed to optimize the combustion chamber of the solid baled biomass. Two different combustion chambers were analysed by distinguishing the air supply in the primary air nozzles. Martin *et al*. (2006) model can be used for selecting the proper steel grade for the shell to prevent slagging and temperature corrosion. The influence of throat angle on the performance of gasifier was studied (Jayah *et al*. 2003) and it was found that the conversion efficiency decreased as the throat angle increased. However, a smaller throat angle needs a longer gasification length for giving maximum efficiency. It is noted that the gasification zone and nozzle inclination are the important parameters to design a gasifier. Sivakumar *et al*. (2008) showed that for getting better species composition, the choke plate designs should be at an angle of 10°- 25°.

Cleition *et al*. (2009) developed a kinetic model by one-step devolatilization and apparent oxidation kinetics with leather waste using CFX 11.0 and showed that the maximum temperature was obtained when homogeneous combustion reactions began. Murugan *et al*. (2016) studied the dimensional suitability of gasifier with different feedstocks such as rice husk, rubber wood, rubber seed kernel shell and coconut shell using the CFD and found out that the species transport model is well suited to predict the composition of producer gas in a downdraft biomass gasifier. The CFD modelling was also used to study the gasification of fluidized bed combustion in a gasifier (Ravi *et al*. (2013)).

From the literature it is observed that the CFD can be a powerful tool to design and analyse the thermo-chemical gasification process. However, the application of CFD in the design and selection of geometrical parameters of downdraft gasifier is not intensively used in the literature. Hence keeping the above aspects, the present work focuses on the simulation of $50kW_{th}$ biomass gasifier with different air nozzle inclination and position by the species transport approach. The predicted results were checked with a few experimental observations, and the validity of the approach is confirmed.

2. Model Description

The schematic diagram of the imbert type biomass downdraft gasifier is shown in Fig. 1. The biomass inlet and gas outlet are having the diameter of 480mm and 430mm respectively. The total height of the gasifier is 2040 mm and the lengths of drying and pyrolysis, combustion and reduction zones are considered as 950mm, 450mm and 480mm respectively.

.

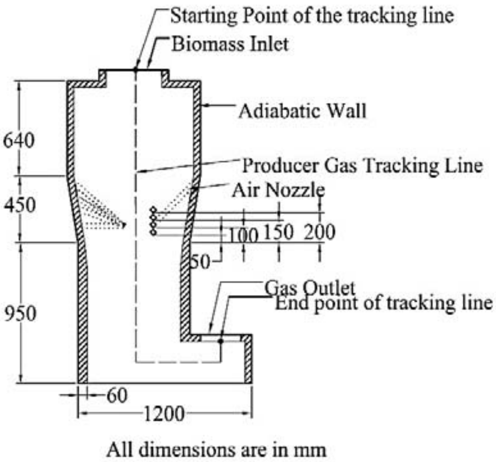

Fig. 1. Description of the downdraft biomass gasifier used in the numerical simulation.

The air nozzle inlet with an inclination of 0°, 20°, 30°, 45° and 60° is designed and the height of the nozzle position is varied at 50mm,100mm, 150mm and 200mm above the reduction zone. The outlet of the air nozzle is alone shown in the two-dimensional model of the gasifier.

3. Numerical Modelling

The two-dimensional model of the biomass downdraft gasifier was drawn in design-modeller and the analysis has been carried out in FLUENT. The detailed numerical modelling procedure is shown in Fig. 2. The governing equations used in this simulation are given in Table 1. The basic assumptions such as homogeneous property, no loss of heat across the wall and chemical reactions are faster than turbulent eddies have been considered to reduce the complexity. Due to the accuracy over the turbulent flows, the RNG k- ε model is used due to higher and lower grade Reynolds number present in this simulation. The homogeneous and heterogeneous reactions in a gasifier are modelled by linking all the four zones so that the output of the first will be the input for the following zone. The gasification reactions involved in this simulation are listed in Table 2. In the eddy dissipation model, the turbulence mixing concept of the species is followed. The SIMPLE algorithm is used to contribute the stable solution of the 2D domain with 2, 93,000 nodes. The species concentration of producer gas is calculated by the eddy dissipation model.

Table 1 Governing equations used in this simulation

Description	Eq No	Ref.
Equation of Mass $\nabla.(\rho\vec{v}) = S_m$	(1)	Luc et al (2008)
Equation of Momentum $\nabla.(\rho\vec{v}\vec{v}) = -\nabla P + \nabla.(\bar{\bar{\tau}}) + \rho\vec{g} + \vec{F}$	(2)	Luc et al (2008)
Equation of Energy $\nabla.(v(\rho E + p)) = \nabla.(\lambda_{eff}\nabla T - \sum hjJj + (\vec{\tau}_{eff}.\vec{v})) + S_h$	(3)	Luc et al (2008)
The turbulence model of the reaction in this work is k-ε RNG model, $C_{1\varepsilon} = 1.44$, $C_{2\varepsilon} = 1.92$, $Y_m = 0.09$,$S_k = 1.0$, $S_e = 1$	(4)	Orzag et al (1993)
$\frac{\partial}{\partial xi}(\rho k u_i) = \frac{\partial}{\partial xj}\left[\left(\mu + \frac{\mu}{\sigma_k}\right)\frac{\partial k}{\partial x_j}\right] + G_k + G_b - \rho\varepsilon - Y_m + S_k$		
The species transport model reaction is noted as		
$\frac{\partial}{\partial t}(\rho Y_x) + \nabla(\rho\vec{v}Y_x) = -\nabla.\vec{J_x} + R_x$	(5)	Magnussen et al (1976)
$R_{i,r} = v'_{i,r}M_{i,r}A\rho\frac{\varepsilon}{k}min_R\left(\frac{Y_r}{v'_{R,r}, M_{w,}}\right)$	(6)	Magnussen et al (1976)
$R_{i,r} = v'_{i,r}M_{i,r}B\rho\frac{\varepsilon}{k}\left(\frac{\sum_p Y_p}{\sum_j^N v''_{j,r}M_{w,j}}\right)$ A= an empirical constant equal to 4.0, B = an empirical constant equal to 0.5	(7)	Magnussen et al (1976)

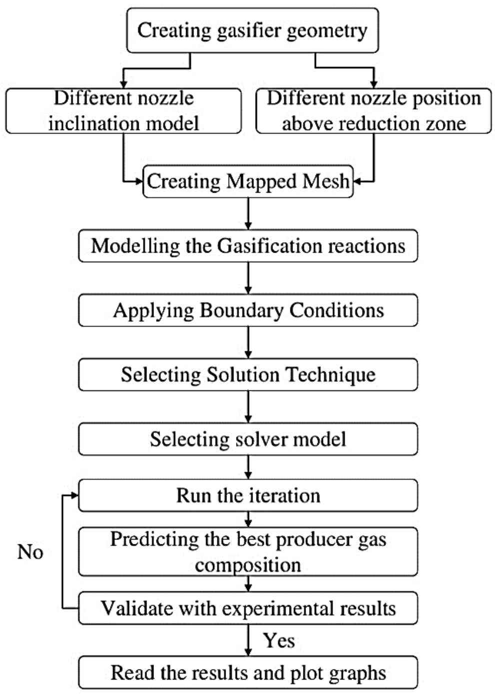

Fig. 2. Flowchart of the numerical simulation.

Table 2 Homogeneous and heterogeneous reactions for gasification

Sl. No	Reactions	Pre-exponential factor (sec^{-1})	Activation Energy (Jkg mol)	Ref
1	$H_2O(l) \rightarrow H_2O(v)$	$5.3 \times e^{10}$	$88 \times e^{03}$	Franciso et al. (2008)
2	$C + O_2 \rightarrow CO_2$	$93.5 \times e^{03}$	$82.8 \times e^{03}$	Andrew et al. (2010)
3	$2CO + O_2 \rightarrow 2CO_2$	$10 \times e^{17}$	$166.28 \times e^{03}$	Franciso et al. (2008)
4	$CH_4 + 1.5\ O_2 \rightarrow CO + 2H_2O$	$92 \times e^{05}$	$80.23 \times e^{03}$	Franciso et al. (2008)
5	$2H_2 + O_2 \rightarrow 2H_2O$	$10 \times e^{11}$	$42 \times e^{03}$	Franciso et al. (2008)
6	$C + H_2O \rightarrow CO + H_2$	$14 \times e^{07}$	$179.50 \times e^{03}$	Andrew et al. (2010)
7	$C + CO_2 \rightarrow 2CO$	$34 \times e^{06}$	$179.50 \times e^{03}$	Andrew et al. (2010)
8	$C + 2H_2 \rightarrow CH_4$	$4.189 \times e^{-03}$	$19.21 \times e^{03}$	Avdhesh Kr Sharma (2008c)
9	$CH_4 + H_2O \rightarrow CO + 3H_2$	$16.50 \times e^{10}$	$33.90 \times e^{07}$	Luc et al. (2008)
10	$CO + H_2O \rightarrow CO_2 + H_2$	$28.24 \times e^{-03}$	$32.840 \times e^{03}$	Ningbo et al. (2008)

3.1 Species Transport Model

The species such as C, O_2, N_2, CO, CO_2, H_2O, CH_4 and H_2 involved in the gasification process are listed in Table 2. The chemical reactions are solved by the conservation equations linking convection, diffusion and reaction of individual species. The general type of the transport equation for each species is given as

$$\partial/\partial t(\rho Y_i) + \nabla.(\rho \vec{v}\ Y_i) = \nabla.\vec{J} + R_i \quad (1)$$

R_i is the net rate of production of species i by gasification reaction. J is the diffusion flux of species i which causes concentration gradients.

Mass diffusion for laminar flows is given as

$$\vec{J} = -(\rho D_{i,m} + \mu_i/Sc_i)\nabla Y_i \quad (2)$$

For turbulent flows, mass diffusion flux is given as

$$\vec{J} = -\rho\ D_{i,m}\ \nabla Y_i \quad (3)$$

where $D_{i,m}$ is the mass diffusion coefficient of species in the mixture, and Sc_i is the turbulent Schmidt number.

So, the transport equations for each chemical species are

$$\frac{\partial}{\partial t}(\rho Y_C) + \nabla(\rho \vec{v}\, Y_C) = -\nabla.\vec{J_C} + R_C \quad (4)$$

$$\frac{\partial}{\partial t}(\rho Y_{O_2}) + \nabla(\rho \vec{v}\, Y_{O_2}) = -\nabla.\vec{J_{O_2}} + R_{O_2} \quad (5)$$

$$\frac{\partial}{\partial t}(\rho Y_{CO_2}) + \nabla(\rho \vec{v}\, Y_{CO_2}) = -\nabla.\vec{J_{CO_2}} + R_{CO_2} \quad (6)$$

$$\frac{\partial}{\partial t}(\rho Y_{CO}) + \nabla(\rho \vec{v}\, Y_{CO}) = -\nabla.\vec{J_{CO}} + R_{CO} \quad (7)$$

$$\frac{\partial}{\partial t}(\rho Y_{N_2}) + \nabla(\rho \vec{v}\, Y_{N_2}) = -\nabla.\vec{J_{N_2}} + R_{N_2} \quad (8)$$

$$\frac{\partial}{\partial t}(\rho Y_{H_2}) + \nabla(\rho \vec{v}\, Y_{H_2}) = -\nabla.\vec{J_{H_2}} + R_{H_2} \quad (9)$$

$$\frac{\partial}{\partial t}(\rho Y_{CH_4}) + \nabla(\rho \vec{v}\, Y_{CH_4}) = -\nabla.\vec{J_{CH_4}} + R_{CH_4} \quad (10)$$

$$\frac{\partial}{\partial t}(\rho Y_{H_2O}) + \nabla(\rho \vec{v}\, Y_{H_2O}) = -\nabla.\vec{J_{H_2O}} + R_{H_2O} \quad (11)$$

$$\frac{\partial}{\partial t}(\rho Y_{H_2O(l)}) + \nabla(\rho \vec{v}\, Y_{H_2O(l)}) = -\nabla.\vec{J_{H_2O(l)}} + R_{H_2O(l)} \quad (12)$$

3.2 Reaction Rate Model

The net rate of production or destruction of species i as the result of reaction r,$R_{i,r}$, is given by the smaller of the two expressions below.

$$R_{i,r} = v'_{i,r} M_{i,r} A\rho \frac{\varepsilon}{k} \min_R \left(\frac{Y_r}{v'_{R,r}, M_{w,j}}\right) \quad (13)$$

$$R_{i,r} = v'_{i,r} M_{i,r} B\rho \frac{\varepsilon}{k} \left(\frac{\sum_p Y_p}{\sum_j^N v''_{j,r} M_{w,j}}\right) \quad (14)$$

where,

Y_p is the mass fraction of any product species, P

Y_r is the mass fraction of a particular reactant, R

3.3 Boundary Conditions

The biomass inlet at the top of the gasifier is defined as mass flow inlet. The producer gas leaving the gas outlet is defined as pressure outlet. The wall of the gasifier is considered as wall boundary with no-slip condition. The ultimate and the proximate analyses of the feedstock used in this simulation are shown in Table 3. It is very difficult to obtain a solution for a simulation which deals with combustion oriented eddy dissipation model. So, a false time stepping has been followed for the turbulence-chemistry interaction. The relaxation factor of 0.01 is used for the calculation of species concentration of producer gas.

Table 3 Proximate and Ultimate analysis of Rubber seed Kernel Shell from Christus *et al.* (2014b)

Proximate Analysis (% w.b.)				
VM	FC	MC		Ash
89.4	6.1	4.3		0.2
Ultimate Analysis (% w.b.)				
C	H	O	N	S
43.2	6.0	0.55	50.25	0

4. EXPERIMENTAL DESCRIPTION

The schematic view of the experimental setup used in this study is shown in Fig 3. The biomass and the generated producer gas move in the downward direction. The air required as per the equivalence ratio is sent through the air blower, and it is supplied to the header. From the header, the air passes through the air nozzles inclined at 45°. The air flow was measured by the orifice meter. The reduction zone was filled with charcoal initially, and the combustion was initiated through the air nozzle. The temperatures on the different zones of the gasifier are measured with calibrated K-type (Chromel-Alumel) thermocouples and recorded by the data logger. The leakage of the producer gas

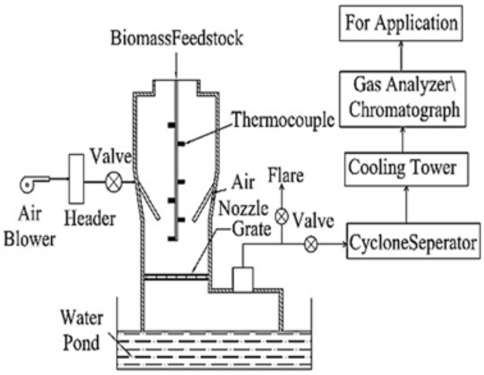

Fig. 3. Experimental Setup of the downdraft biomass gasifier.

is prevented by the water tank available at the bottom of the gasifier. A gas chromatograph (NUCON 5765) is used to measure the composition of producer gas. Gas samples are collected in air tight syringe for various operating conditions and analyzed in the gas chromatograph with argon as carrier gas.

4.1 Experimental Procedure

The gasifier was initially loaded with a known quantity of rubber seed kernel shell with a moisture content of 10-15%. The water tray of the gasifier was filled with water and the biomass feed door was closed to prevent the leakage of producer gas. The air blower is used to supply air through one of the nozzles. Gate valves are used for this purpose. A red-hot charcoal was inserted through the air nozzle to start the combustion process, and the effective combustion inside the gasifier starts after 10 minutes. The temperature is recorded by data logger with the K-type thermocouple.

The ash and the char residues left out after the combustion are passed through the grate once it is shaken by the lever. The ash generated in the experiments is collected at the bottom of the water tray and it is weighed. An online gas analyser (Electronic System Tech) is used to compute the purity and higher heating value of the gas generated from the gasifier. The experiment is carried out for the duration of 3hrs and the average values of the producer gas composition, temperature distribution, and higher heating value of the gas are noted. Mass balance of the gasifier was noted to explore the consistency of the results produced. The air flow rate and biomass consumption rate are considered as input, and the producer gas generated and the ash collected are taken as output. The mass balance for the rubber seed kernel shell as feedstock is given in Table 4.

Table 4 Mass balance for the rubber seed kernel shell as feedstock

Run	Nozzle Position(mm)	Air flow rate (m^3/h)	Input		Output		Mass Balance (%)
			Air flow rate (kg/h)	Biomass consumption rate (kg/h)	Producer gas flow rate (kg/h)	Char Collected (kg/h)	
1.	20	14	16	8	22	1.5	93
2.	45	14	16	9	24	2.2	95

5. RESULT AND DISCUSSION

From the post-processing facility of the software, the species concentration of producer gas along the various zone has been taken by collecting the data from all the points on the tracking line as shown in Fig 1. The species concentrations and higher heating value of the selected cells are imported to Excel software and further used to analyze the performance of the gasifier. The analysis has been carried out for different air nozzle inclination and position of the air nozzle above the reduction zone with rubber seed kernel as feedstock and equivalence ratio as 0.25.

5.1 Validation of the Numerical Model

The composition of combustible gases such as CO, H_2 and CH_4 of the producer gas reported in the previous studies has been compared with the numerical results of the present study and is given in Table 5. In the referred studies, woody biomasses are used with moisture content and equivalence ratio close to the present study.

Table 5 Validation of the numerical work with literature results

Sl. No.	References	Type of Study	Producer Gas Composition		
			CO	H_2	CH_4
1.	Fletcher *et al*.(2000)	N	0.10	0.20	0.01
		E	0.16	0.10	0.01
2.	Zainal *et al*. (2001)	A	0.19	0.21	0.06
		E	0.23	0.15	0.01
3.	Jayah *et al*. (2003)	A	0.18	0.13	0.01
		E	0.19	0.15	0.01
4.	Jarungtham machote *et al*. (2007)	E	0.19	0.16	0.01
5.	Chirstus *et al*. (2015)	A	0.19	0.14	0.01
		E	0.23	0.16	0.01
6.	Murugan *et al*. (2016)	N	0.24	0.15	0.01
		E	0.23	0.16	0.01
7.	Present Work (2016)	N	0.23	0.16	0.02
		E	0.22	0.15	0.01

N – Numerical E – Experimental
A - Analytical

The Experimental (E), Analytical (A) and Numerical (N) results given in Table 5 show that the deviations of the predicted results are within ± 5%, which might be due to some assumptions like homogenous property, no heat loss across the wall, chemical reactions are faster than the turbulent eddies with no slip condition, etc. used in this simulation. Thus, the validity of the present approach has been proved.

5.2 Angle of Nozzle and its Performance

The species concentration of the producer gas for different inclinations is given in Fig. 4. It is observed that at the nozzle angle of 45°, the velocity distribution is uniform throughout the volume, and therefore the major reactions required to form the better composition of combustible gases are highly possible. The figure shows that the composition of CO is 23% at this angle which is due to high conversion of CO_2 to CO and the limited supply oxygen to the combustion zone. The species concentration of H_2 is normally influenced by water-gas shift reactions. When the nozzle angle is 45° the potential of water-gas shift reactions is high because of the uniform distribution of the reacting compounds in the reduction zone, and the maximum composition of H_2 observed is 17%. Moreover, this high percentage is also due to the limited supply of O_2 which reduces the H_2O conversion in the combustion zone. The methane generation is uniform for all the nozzle angles which may be due to the stable methane reforming reaction, and the composition, observed are similar to the results reported in the previous studies (Fletcher *et al*. (2000)). The air flow rate is an important input parameter for the control of N_2 in the gasifier. All the N_2 sent to the gasifier may not be available in the producer gas, and this is due to the formation of NOx inside the gasifier, and it is seen that the different nozzle angles have more or less the same amount of N_2 in the output region, which is on par with the results reported in the literature (Jayah *et al*. (2003)). Experiments have been conducted for 20° and 45° nozzle angles, and the results show that the predicted values are close to the experimental results at 45° nozzle angle.

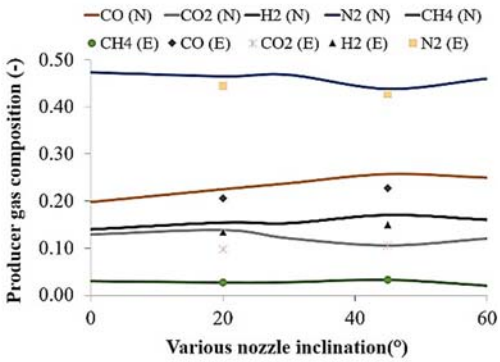

Fig. 4. Producer gas composition for different air nozzle inclination.

Further increase of nozzle angle above 45° decreases the combustible gas composition of the producer gas.

5.3 Position of Nozzle and its Performance

From the observed results, it is predicted that 45° nozzle inclination is suitable for the imbert type downdraft biomass gasifier. Hence keeping the 45° inclination as constant, the nozzle position is varied from 50mm - 200mm above the length of the reduction zone. From the results shown in Fig. 5, it is predicted that the nozzle position at a height of 100mm above the reduction zone yields better gas concentration when compared with the other air nozzle positions. At 100mm position, the air nozzle lies on the middle of the combustion zone, and the length of the reduction zone is more than 1000mm and yields more producer gas concentration due to high temperature at the entry of the reduction zone. The water-gas shift reactions and methane reforming reactions are maximum at 100mm position and this reduces the formation from CO to CO_2.

The change in nozzle position either disturbs the length of the reduction zone or maintains the temperature in the pyrolysis zone. The insufficient length of reduction zone could not complete the reactions in the reduction zone which leads to low composition of combustible gases in the producer gas. If the combustion zone is shifted towards the drying zone by moving the nozzle, the pyrolysis reaction potential is reduced and also the thermal energy required in the reduction zone may not be supplied with appropriate temperature to carry out the endothermic reactions.

Experiments were also conducted for each nozzle position, and the gas samples are tested through gas chromatograph (NUCON 5765). The variations in gas composition observed from the experiments are similar to the predicted results. This proves that the length of the reduction zone plays an active role in the design of downdraft biomass gasifier.

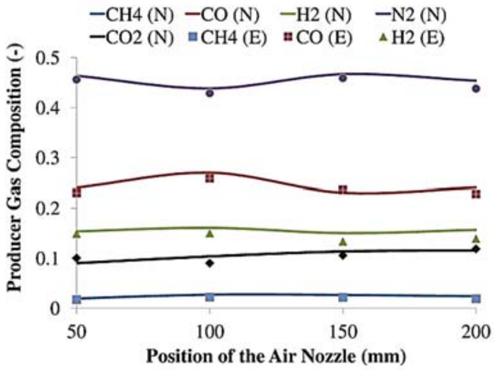

Fig. 5. Producer gas composition for different nozzle position.

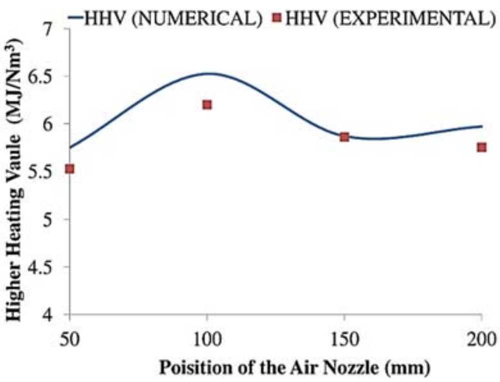

Fig. 6. Higher heating value for different nozzle position.

5.4 Higher Heating Value

The main components which are responsible for the higher heating value of the producer gas are carbon monoxide, hydrogen and methane. When the nozzle position is 100 mm above the reduction zone, the maximum Higher Heating Value (HHV) of 6.5 MJ/Nm^3 is observed and further change in position decreases the HHV. This is due to the presence of the inert gas nitrogen and moisture in feedstock. When the nozzle is shifted towards the drying zone, due to lack of reactions at pyrolysis and reduction zones, the combustible gas composition is reduced which leads to lower heating value of the producer gas at nozzle position above 100 mm. The numerical results plotted in Fig. 6 also show that the values are close to the experimental observation. Therefore, the nozzle exit at 100mm above the reduction zone with an inclination of 45° has been identified as the best arrangement of air nozzle.

5.5 Temperature Distribution

Figure 7 shows the variation of average temperature along the various zones of the downdraft biomass gasifier with nozzle arrangement of 45° inclination and position at 100 mm above the reduction zone.

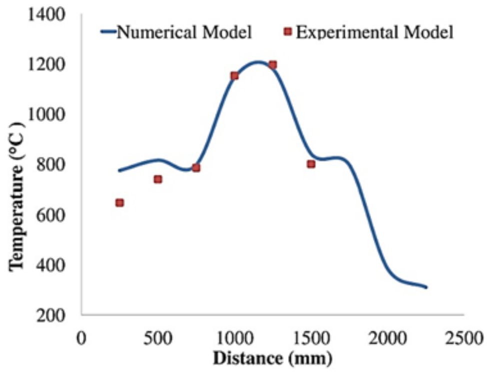

Fig. 7. Temperature distribution for 45° nozzle inclination and 100 mm nozzle position.

The temperature of the combustion zone varies from 820°C to 1197°C when the drying zone is close to 600°C. The maximum temperature is achieved by the combustion zone due to the release of heat from the burnt products. The gas leaving through the gas outlet shows 275°C.When the air flow rate is further increased, the mass flow rate of N_2 increases which reduces the temperature of the combustion and reduction zones. This reduction in temperature affects the potential of the reduction zone reactions. Therefore, a proper temperature distribution is needed throughout the gasifier for a better efficiency. Since the temperature distribution shown in Fig. 7. is close to the suitable temperature needed for optimum performance of the gasifier (Chirstus *et al*. (2014b)), the proposed numerical approach is validated.

6. CONCLUSION

The influence of the position and the inclination of air nozzle on the performance of a 50kWth biomass gasifier has been studied, and the results obtained from CFD analysis and experimental observations for the feedstock rubber seed kernel shell leads to the following conclusions.

- The k-ε RNG model can be used to simulate the biomass gasification in a downdraft gasifier.
- Among the different nozzle inclinations studied, the optimum species concentration of the producer gas is obtained at 45°. It is also observed that the nozzle inclination is having a greater impact on the performance of the gasifier. Lower the inclination angle of air nozzle gives poor quality of producer gas.
- The higher heating value of the producer gas obtained from simulation is ranging from 5 to 6 MJ/Nm^3 for an equivalence ratio of 0.25. It is

also observed that the HHV is maximum when the nozzle position is kept at 100mm above the reduction zone.

- The temperature profile obtained from both experimental and numerical results shows a similar trend.
- The concentrations of CO, CO_2, H_2, CH_4 and N_2 in the producer gas predicted from the numerical study are 23%, 11%, 14%, 2% and 45% respectively. These values are close to the experimental results which prove the validity of the numerical approach used in the study.

ACKNOWLEDGEMENTS

The authors would like to acknowledge the "All India Council for Technical Education (AICTE), India" for providing the financial support through a sponsored research project under the reference 20/AICTE/RIFD/RPS / (POLICY-1)17/2013-14.

REFERENCES

Altafini, C. R., P. R. Wander and R. M. Barreto (2003). Prediction of the working parameters of a wood waste gasifier through an equilibrium model. *Energy Conversion and Management* 44, 2763-2777.

Arnavat, M. P., J. C. Bruno and A. Coronas (2010). Review and analysis of biomass gasification models. *Renewable and Sustainable Energy Reviews* 14, 2841-2851.

Babu, B. V. and P. N. Sheth (2006). Modelling and simulation of reduction zone of downdraft biomass gasifier: Effect of char reactivity factor. *Energy Conversion and Management* 47, 2602-2611.

Christus, J. S. V. and S. J. Sekhar (2016). Performance studies on a downdraft biomass gasifier with blends of coconut shell and rubber seed shell as feedstock. *Applied Thermal Engineering* 97, 22-27.

Christus, J. S. V., K. Thyagarajan, P. C. Murugan and S. J. Sekhar (2014). Rubber Seed Kernel as a Substitute for Wood in a Biomass Gasifier-An Experimental Study. *Advanced Materials Research* 984-985, 845-849.

Christus, J. S. V., S. J. Sekhar and K. Thygarajan (2014). Performance studies on downdraft gasifier with biomass energy sources available in remote villages. *American Journal of Applied Sciences* 11 (4), 611-622.

Fletcher, D. F., B. S. Haynes, F. C. Christo and S. D. Joseph (1997). Combustion modelling for an entrained flow biomass gasifier. *International Conference on CFD in mineral and metal processing and power generation, CSIRO, Melbourne.*

Fletcher, D. F., B. S. Haynes, F. C. Christo and S. D. Joseph (2000). A CFD based combustion model of an entrained flow biomass gasifier. *Applied Mathematical Modelling* 24, 165-182.

Gao, N. and A. Li (2008). Modelling and Simulation of Combined pyrolysis and reduction zone for a downdraft biomass gasifier. *Energy Conversion and Management* 49, 3483-3490.

Gerun, L., M. Paraschiv, R. Vijeu, J. Bellettre, M. Tazerout, B. Gobel and Ulrikhenriksen (2008). Numerical investigation of the partial oxidation in a two-stage downdraft gasifier. *Fuel* 87, 1383-1393.

Hsi, C. H., T. Y. Wang, C. H. Tsai, C. Y. Chang, C. H. Liu, Y. C. Chang and J. T. Kuo (2008). Characteristics of an air-blown fixed-bed downdraft biomass gasifier. *Energy & Fuels* 22(6), 4196-4205.

Jaojaruek, K. and S. Kumar (2009). Numerical simulation of the pyrolysis zone in a downdraft gasification process. *Bio Resource Technology* 100, 6052-6058.

Jarungthammachote, S. and A. Dutta (2006). Thermodynamic equilibrium model and second law analysis of downdraft waste gasifier. *Energy* 32, 1660-1669.

Jayah, T. H., L. Aye, R. J. Fuller and D. F. Stewart (2003). Computer simulation of a downdraft wood gasifier for tea drying. *Biomass and Bioenergy* 25, 459-469.

Laurence, L. C. and D. Ashenafi (2012). Syngas Treatment Unit for Small Scale Gasification - Application to IC Engine Gas Quality Requirement. *Journal of Applied Fluid Mechanics* 5, 1, 95-103.

Li, B., H. Chen, H. Yang, X. Wang and S. Zhang (2013).Characteristics of the temperature distribution and product gas evolving of an updraft biomass gasifier. *Energy & Fuels* 27(3), 1460-1465.

Magnussen, B. F. and B. H. Hjertager (1976). On mathematical models of turbulent combustion with emphasis on soot formation and combustion. *16th International Symposium on Combustion, Combustion Institute, Pittsburgh*.

Miltner, M., A. Markaruk, M. Harasek and A. Fridel (2006). CFD-Modelling for the combustion of solid baled biomass. *Fifth International Conference on CFD in the process industries, CSIRO, Australia.*

Murugan, P. C. and S. J. Sekhar (2016). Numerical simulation of imbert biomass gasifier to select the feedstock available in remote areas. *Environmental Progress and Sustainable Energy*.

Orszag, S. A., V. Yakhot, W. S. Flannery, F. Boysan, J. C. Maruzewski and B. Patel (1993).

Renormalization group modelling and turbulence simulations. *International conference on Near Wall turbulent* flows, Tempe, Arizona.

Patel, K. D., N. K. Shah and R. N. Patel (2013). CFD analysis of spatial distribution of various parameters in downdraft gasifier. *Procedia Engineering* 51,764-769.

Porciuncula, C. B., N. R. Marcilio, M. Godinho and A. R. Seechi (2009). Fluid dynamics for design of a biomass gasifier.*10th International symposium on Process Systems Engineering, Brazil* 1071-1076.

Sandamali, D., Gunarathne, A. Mueller, S. Flecks, T. Kolb, J. K. Chmielewski, W. Yang and W. Blasiak (2014). Gasification characteristics of hydrothermal carbonized biomass in an updraft pilot scale gasifier. *Energy & Fuels* 28(3), 1992-2002.

Sharma, A. K., (2008a). Equilibrium modelling of global reduction reactions for a downdraft gasifier (biomass) gasifier. *Energy Conversion and Management* 49, 832-842.

Sharma, A. K. (2008b). Equilibrium and kinetic modelling of char reduction reactions in a downdraft biomass gasifier: A Comparison. *Solar Energy* 82, 918-928.

Sharma, A. K. (2011). Modelling and simulation of a downdraft gasifier1. Model development and validation. *Energy Conversion and Management* 52, 1386-1396.

Singh, R. I., A. Brink and M. Hupa (2013). CFD modelling to study fluidized bed combustion and gasification. *Applied Thermal Engineering* 52, 585-614.

Sivakumar, S., K. Pitchandi and E. Natarajan (2008). Modelling and simulation of downdraft wood gasifier. *Journal of Applied Sciences* 8(2), 271-279.

Slezak, A., J. M. Kuhlam, L. J. Shadle, J. Spenik and S. Shi (2010). CFD simulation of entrained-flow coal gasification: Coal particle/size fraction effects. *Powder Technology* 203, 98-108.

Tinaut, F. V., A. Melgar, J. F. Perez and A. Horrillo (2008). Effect of biomass particle size and air superficial velocity on the gasification process in a downdraft fixed bed gasifier. An experimental and modelling study. *Fuel Processing Technology* 89, 1076-1089.

Wang, Y. and L. Yan (2008). CFD studies on biomass thermochemical conversion. *International Journal of Molecular Sciences* 9, 1108-1130.

Yang, Y. B., V. N. Sharifi and J. Swithenbank (2005). Numerical simulation of the burning characteristics of thermally thick biomass fuels in packed beds. *Process Safety and Environmental Protection* 83, (B6), 549-558.

Yang, Z., Z. Wang, Y. Wu, J. Wang, J. Lu, Z. Li and W. Ni (2011). Dynamic for an oxygen-staged slagging entrained flow gasifier. *Energy & Fuels* 25(8), 3646-3656.

Yuehong, Z., W. Hao and Xuzhihong (2006). Conceptual design and simulation study of a co-gasification technology. *Energy Conversion and Management* 47, 1416-1428.

Zainal, Z. A., R. Ali, C. H. Lean and K. N. Seetharamu (2001). Prediction of performance of a downdraft gasifier using equilibrium modelling for different biomass materials. *Energy Conversion and Management* 42, 1499-1515.